해부 · 생물인류학 제 38 권 제 3 호
Anat Biol Anthropol Vol. 38, No. 3 (2025) pp. 255~262
https://doi.org/10.11637/aba.2025.38.3.255

Original Article

An Anatomical Spectrum of Ciliopathy in Jbts17 Knockout Mice: Craniofacial Dysmorphology, Polydactyly and Forebrain Anomalies

Hyowon Hong[1]

[1]*Research Affairs, Keimyung University Dongsan Medical Center*

Abstract : Primary cilia orchestrate key developmental signaling pathways, and their dysfunction causes multisystem disorders collectively termed ciliopathies that often present with structural anomalies of the face, limbs, and brain. JBTS17 encodes a cilia associated scaffold required for proper ciliogenesis and ciliary signaling. Biallelic loss-of-function variants in JBTS17 are linked to Joubert spectrum disorders that include craniofacial malformations and polydactyly. To delineate the anatomical consequences of complete gene inactivation in vivo, we generated a CRISPR/Cas9 induced frameshift null allele of the murine Jbts17 locus. Late gestation *Jbts17*^{KO} embryos showed ocular hypopigmentation with shallow optic cups, anterior craniofacial dysmorphology, and autopod polydactyly. Coronal brain sections revealed reduced cortical thickness with apparent ventriculomegaly, and the olfactory nerve was bilaterally absent at the level of the fila olfactoria. Mouse embryonic fibroblasts derived from knockout embryos displayed reduced Lis1 protein, consistent with a link between Jbts17 loss and Lis1 dependent cellular processes. These findings indicate that Jbts17 supports cilia dependent regional patterning in eye, craniofacial, and distal limb development and contributes to forebrain and olfactory development. The Jbts17 knockout provides a practical model of ciliopathy associated structural and neuroanatomical anomalies and an anatomical reference for subsequent quantitative and mechanistic studies.

Keywords : Jbts17, Primary cilia, Craniofacial malformation, Polydactyly, Olfactory nerve agenesis, Forebrain anomaly

INTRODUCTION

Primary cilia are solitary microtubule-based organelles that relay key developmental signals, including Hedgehog, Wnt/planar cell polarity, and PDGFRα [1-3]. Perturbation of ciliogenesis or ciliary signaling produces a spectrum of multisystem disorders known as ciliopathies, marked by regional structural anomalies of the craniofacial complex, limb patterning, and the central nervous system [4-6]. From an anatomical perspective, craniofacial malformations reflect altered growth and fusion of the frontonasal and maxillary prominences; limb anomalies, classically polydactyly, arise from disturbed Hedgehog-GLI processing in the developing autopod [7]; and forebrain findings such as cortical plate thinning and defects of the olfactory system underscore the contribution of cilia mediated signaling to progenitor dynamics, radial expansion, and axon projection pathways [8-11].

The author(s) agree to abide by the good publication practice guideline for medical journals.
The author(s) declare that there are no conflicts of interest.
Received: September 7, 2025; **Revised:** September 18, 2025; **Accepted:** September 21, 2025
Correspondence to: Hyowon Hong (Research Affairs, Keimyung University Dongsan Medical Center, Daegu 42601, Republic of Korea)
E-mail: cnsl428@dsmc.or.kr

ISSN 2671-566X (Online)

JBTS17/CPLANE1 encodes a cilia associated scaffold required for proper ciliogenesis and ciliary signal transduction [12]. Consistent with this role, JBTS17 localizes to the basal body of the primary cilium (the distal end of the mother centriole), and siRNA mediated depletion reduces the fraction of ciliated cells and axoneme length in cultured cells [13]. Clinically, biallelic loss-of-function variants in JBTS17 underlie subsets of the Joubert spectrum and oral facial digital syndrome type VI, in which craniofacial dysmorphology, polydactyly, and variably penetrant ocular and forebrain abnormalities are reported [14-16]. Patient derived cells with JBTS17 variants show hypomorphic ciliogenesis with reduced ciliation, shortened primary cilia, and attenuated Hedgehog target induction, consistent with combined structural and signaling defects [14,17,18].

Beyond its ciliary role, prior studies including our own have linked JBTS17 to cytoskeletal programs relevant to mitosis and migration, suggesting points of intersection between ciliary and nonciliary mechanisms during embryogenesis [13]. In particular, we previously reported that JBTS17 depletion lowers LIS1 (PAFAH1B1) protein and impairs neuronal migration during corticogenesis, implicating a JBTS17-LIS1 axis in neurodevelopment.

Here, we report an anatomical analysis of a CRISPR/Cas9 induced frameshift null allele of the murine Jbts17 locus. Focusing on late gestation embryos, we observe ocular hypopigmentation with optic cup shallowing, anterior craniofacial dysmorphology (midface flattening with narrowed external nares), and autopod restricted polydactyly, while overall somatic size is preserved. In the forebrain, cortical plate thinning with qualitative ventriculomegaly is evident on coronal sections despite comparable gross telencephalic contours, and the olfactory nerve (cranial nerve I) is bilaterally absent at the level of the fila olfactoria. At the cellular level, Lis1 protein is reduced in Jbts17 null mouse embryonic fibroblasts, extending our earlier knockdown observations to a germline knockout context.

Collectively, these findings indicate that Jbts17 supports cilia dependent regional patterning across eye, craniofacial, and limb development and contributes to forebrain and olfactory development at late gestation. The Jbts17 knockout thus provides a practical model that couples clear anatomical readouts with a cell level marker (Lis1 reduction), offering an integrated framework for future quantitative and mechanistic dissection of JBTS17 related ciliopathy pathogenesis.

MATERIALS AND METHODS

1. Generation of Jbts17 knockout mice

A germline loss-of-function allele of Jbts17 was generated by CRISPR/Cas9-mediated mutagenesis. Guide RNAs targeting exon 3 of the mouse Jbts17 locus were synthesized by in vitro transcription and co-injected with Cas9 mRNA into C57BL/6 blastocysts, which were subsequently transferred to pseudopregnant foster mothers. Founder animals were genotyped by Sanger sequencing, and two independent early frameshift alleles (c.64_76del and c.71_74del) were recovered. Heterozygous animals were intercrossed to generate homozygous mutants and wild-type littermates for analysis. All animal procedures were performed in accordance with institutional guidelines and approved by the Institutional Animal Care and Use Committee.

2. Embryo collection and gross anatomical examination

Timed matings were established, and embryos were harvested at embryonic day 18 (E18) by maternal sacrifice. Whole-mount embryos were inspected for crown-rump length, ocular pigmentation, craniofacial morphology, and limb patterning. Images were obtained using a stereomicroscope equipped with a digital camera. Postnatal day 0 (P0) pups were also examined for craniofacial and limb phenotypes.

3. Histology and brain sectioning

Whole embryonic brains were dissected in cold phosphate-buffered saline (PBS), immersion-fixed in 4% paraformaldehyde overnight, and cryoprotected in 30% sucrose. Tissues were embedded in optimal cutting temperature compound and sectioned coronally at 25 μm using a cryostat. Sections were mounted on glass slides and stained with hematoxylin and eosin or imaged under brightfield optics. Cortical thickness and ventricular morphology were assessed at matched rostrocaudal levels.

4. Mouse Embryonic Fibroblast (MEF) preparation and immunoblotting

MEFs were prepared from E18 embryos by standard trypsin dissociation. Cells were cultured in Dulbecco's modified Eagle medium (DMEM) supplemented with 10% fetal

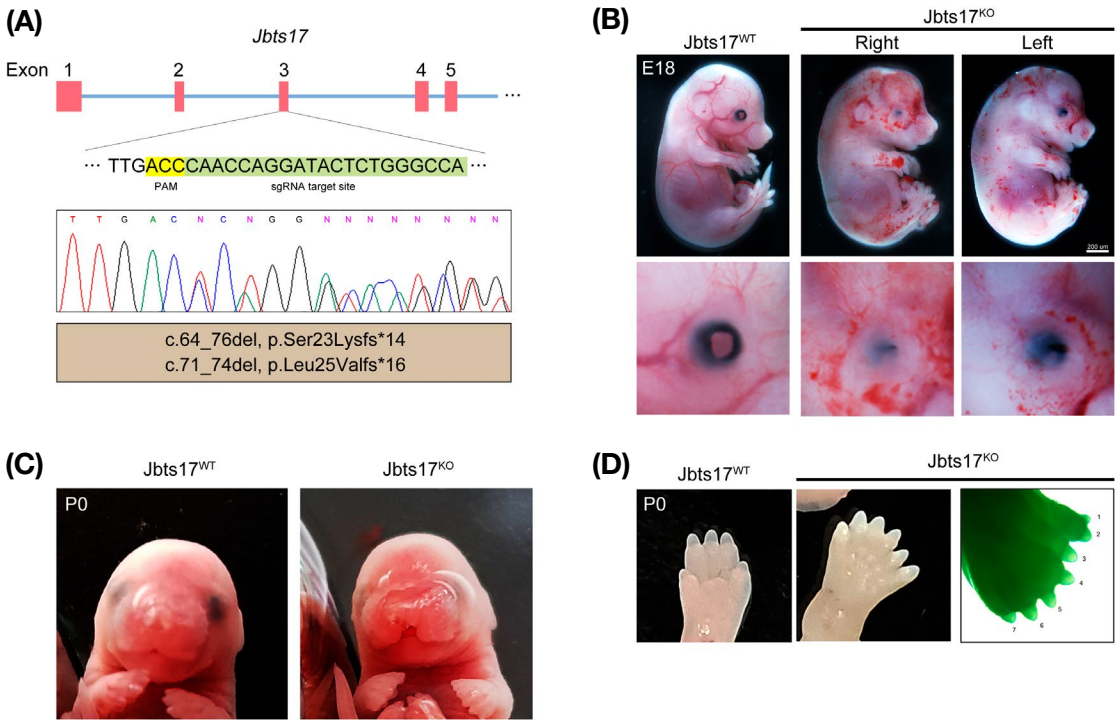

Fig. 1. Generation of a Jbts17 knockout mouse model exhibiting craniofacial and retinal dystrophy with polydactyly. (A) Schematic diagrams showing CRISPR/Cas9 strategy targeting exon 3 of Jbts17. Two independent early frameshift alleles were recovered by Sanger sequencing: c.64_76del (p.Ser23Lysfs*14) and c.71_74del (p.Leu25Valfs*16), each introducing a premature stop early in the N-terminal region. (B) E18 whole-mount views. *Jbts17*^{KO} embryos show reduced ocular pigmentation with a shallow/indistinct optic cup relative to wild type. (C) P0 craniofacial views. *Jbts17*^{KO} embryos display anterior craniofacial dysmorphology, including midface flattening and narrowed, irregular external nares, consistent with involvement of derivatives of the frontonasal and maxillary prominences. (D) P0 hindfeet. Autopods from *Jbts17*^{KO} pups exhibit polydactyly.

bovine serum, 100 U/mL penicillin, and 100 µg/mL streptomycin. Protein lysates were prepared using RIPA buffer with protease and phosphatase inhibitors. Equal amounts of protein were resolved by SDS-PAGE, transferred to nitrocellulose membranes, and immunoblotted with antibodies against Lis1 (PAFAH1B1) and GAPDH as a loading control. Signals were visualized by enhanced chemiluminescence.

5. Imaging analyses

Whole-mount embryos were photographed using a Samsung Galaxy smartphone camera under ambient laboratory lighting without additional optical devices. Coronal brain sections were imaged with a Olympus stereomicroscope. Images were processed with ImageJ software. For qualitative comparisons, sections were matched by anatomical landmarks. No quantitative morphometrics or pathway readouts (e.g., Gli1, Ptch1, GLI3 isoforms) were performed in this study.

RESULTS

1. Biallelic Jbts17 loss disrupts ocular and craniofacial development in late-gestation embryos

To establish a germline loss-of-function allele of *Jbts17*, we used CRISPR/Cas9 microinjection strategy targeting exon 3 (Fig. 1A). Single-guide RNAs (sgRNAs) and Cas9 mRNA were synthesized by in vitro transcription, purified, and co-injected into blastocysts, which were then transferred to surrogate dams by embryo transfer. Genotyping of pups by Sanger sequencing identified two independent early frameshift alleles, c.64_76del (p.Ser23Lysfs*14) and c.71_74del (p.Leu25Valfs*16), each introducing a frameshift that generates a premature termination codon early in the N-terminal region of Jbts17 (Fig. 1A). Heterozygous males and females carrying the edited each allele were intercrossed, and late-gestation (E18) litters were collected from timed pregnancies by maternal sacrifice.

At E18, *Jbts17*^{KO} embryos exhibited reduced retinal pigmentation with a shallow/indistinct optic cup contour relative to wild type, with bilateral involvement (Fig. 1B). Although detailed lamination could not be assessed without histology, the extent of hypopigmentation and cup flattening suggested delayed or abnormal retinal development rather than microphthalmia. Clinically, ocular involvement is variably reported in JBTS17 loss-of-function cohorts, including early retinal dysfunction/dystrophy and hypopigmentation within the ciliopathy spectrum [19]; the bilateral hypopigmentation and optic cup shallowing observed here align with these human findings while underscoring the preservation of overall somatic growth often seen prenatally in ciliopathies. In contrast, gross body size, which is assessed by overall appearance and crown-rump length, was comparable between mutants and wild-type littermates, indicating no overt growth restriction at this stage (Fig. 1B).

Beyond the ocular findings, *Jbts17*^{KO} embryos displayed craniofacial dysmorphology, including mid-facial hypoplasia and altered nasal/maxillary contours (Fig. 1B and C). Close views of the external nares showed irregular, narrowed openings in mutants and similar phenotypes persisted at P0. The visible abnormalities localized to derivatives of the frontonasal and maxillary prominences, consistent with regional patterning defects. Without skeletal preparations or cephalometric quantitation, precise morphometrics (e.g., nasal bone length, maxillary arch width) could not be assigned. However, the nares narrowing and midface flattening indicate anterior craniofacial involvement rather than a generalized jaw size reduction. Comparable orofacial anomalies have been documented in JBTS17 loss-of-function patients, including midface hypoplasia and nasal aperture abnormalities, situating the mouse phenotype within the recognized ciliopathy craniofacial spectrum. Together with the preserved body size at E18, these findings support a model in which cilia-dependent regional patterning is compromised while global fetal growth remains largely intact.

2. Jbts17 loss disrupts distal limb patterning in late-gestation embryos, yielding autopod polydactyly

In humans, biallelic JBTS17 loss-of-function variants are associated with limb malformations, most commonly polydactyly, within the Joubert syndrome or Oral-Facial-Digital (OFD) syndrome type VI spectra [16]. Consistent with these clinical observations, at E18 and PO, *Jbts17*^{KO} embryos displayed polydactyly, with supernumerary digit rays extending the distal margin beyond the typical five-digit arrangement (Fig. 1B and D). In the representative embryos shown, the involvement was bilateral but asymmetric, while the proximal segments (stylopod/zeugopod) showed no gross shortening or disproportionality on whole-mount inspection, indicating that the abnormality is confined to the distal limb (autopod). In particular, the tibial (hallux) sector of the foot exhibited a bifid ray in the I-II territory, digits 1 and 2 diverging from a common proximal stalk, whereas the fibular side contained two independent supernumerary rays lateral to digit V (designated 6 and 7) (Fig. 1D). In both autopods, the added rays were separated by distinct interdigital clefts, and the distal contour was broadened toward the fibular margin. Mechanistically, primary cilia on limb-bud mesenchyme are required to interpret Sonic hedgehog (SHH) cues from the zone of polarizing activity, and disruption of ciliogenesis perturbs anteroposterior patterning of the autopod, a canonical route to extra digits [1,20]. Because JBTS17 localizes to the basal body and is required for proper ciliogenesis, loss of Jbts17 would be expected to alter cilia-dependent SHH-GLI signaling during late autopod development. While we did not quantify pathway readouts (e.g., Gli1/Ptch1 expression or GLI3A/GLI3R ratios), the autopod-restricted, bilateral-but-asymmetric pattern observed here is consistent with cilia-mediated limb-patterning defects and aligns with JBTS17 loss-of-function presentations in patients.

3. Cortical thinning with bilateral olfactory nerve agenesis despite preserved telencephalic size in Jbts17-deficient embryos

Previous study has reported that Jbts17 deficiency during embryogenesis reduced cortical thickness with alteration of mitotic progression of neural progenitors [13]. To determine whether this phenomenon is also recapitulated in *Jbts17*^{KO} embryos, we examined the whole brains at E18. Overall telencephalic size and external contour were comparable to wild-type littermates without overt microcephaly or hemispheric disproportionality (Fig. 2A). By contrast, coronal sections at matched rostro-caudal levels revealed a qualitative reduction in cortical thickness within the dorsal telencephalon of mutants, a change not readily appreciable on gross views (Fig. 2B). In the same sections, the lateral

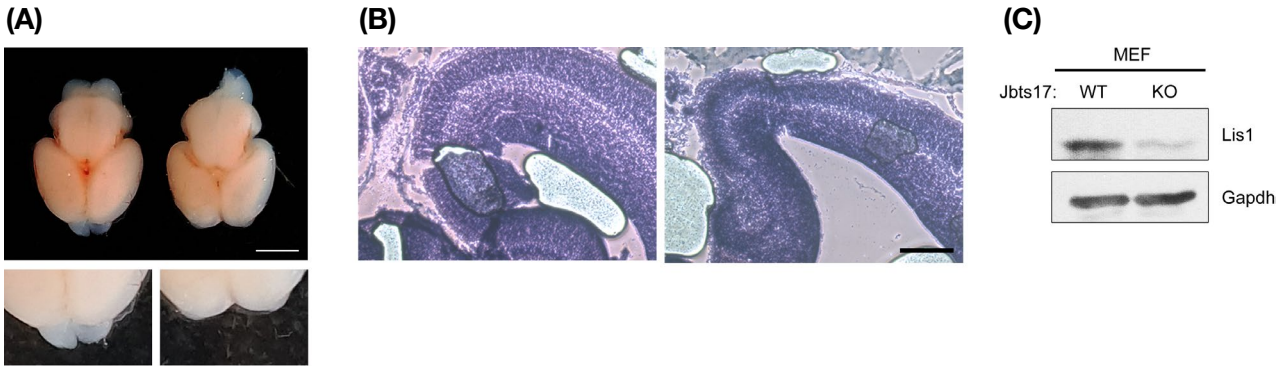

Fig. 2. Forebrain anomalies in Jbts17 deficient embryos. (A) E18 whole mount brains. The olfactory bulbs are not discernible in *Jbts17*^{KO} embryos (bilateral olfactory bulb agenesis), whereas distinct bulbs are evident in wild type. (B) Coronal sections at matched rostro caudal levels. *Jbts17*^{KO} forebrains show reduced cortical plate thickness in the dorsal telencephalon together with an apparent expansion of the lateral ventricular space. (C) Immunoblots showing protein levels of Lis1 in mouse embryonic fibroblasts (MEFs). GAPDH serves as a loading control. Bars, 200 μm.

ventricular space appeared expanded relative ventricular expansion, likely explaining the preserved outer telencephalic contour seen in whole mounts. From an anatomical standpoint, these observations indicate that radial expansion of the cortical mantle is selectively reduced, whereas tangential dimensions are relatively preserved at this stage.

Intriguingly, inspection of the rostral telencephalon revealed no discernible olfactory nerve (cranial verve I) bundles traversing from the nasal cavity toward the forebrain in *Jbts17*^{KO} embryos, whereas bundled fibers were evident in wild-type littermates at E18 (Fig. 2B, below). The absence was bilateral in the representative specimens. Anatomically, the lack of visible fila olfactoria indicates olfactory nerve agenesis at late gestation. Because the olfactory nerve represents primary sensory axons from the olfactory epithelium projecting to the olfactory bulb, this configuration suggests a failure of rostral forebrain-nasal connectivity at or before the stage when axons normally cross the cribriform plate. Unlike the siRNA-mediated knockdown system which was previously used in JBTS17 study, the knockout uncovered bilateral olfactory nerve agenesis. Collectively, the knockout extends prior knockdown observations to a broader neurodevelopmental spectrum, spanning cortical radial growth and olfactory nerve formation, positioning Jbts17 as a key cilia-dependent regulator of late-gestation forebrain development.

4. Jbts17 deficiency reduced Lis1 protein levels in mouse embryonic fibroblasts

LIS1 (PAFAH1B1) is a core regulator of cytoplasmic dynein that governs mitotic spindle positioning, interkinetic nuclear migration, and radial glial polarity [21,22]. In the developing cortex, LIS1 dosage controls progenitor proliferation and neuronal migration, and partial loss yields reduced cortical thickness and lamination defects [13,23]. In the olfactory system, the LIS1-dynein axis supports chain migration of SVZ-derived neuroblasts along the rostral migratory stream to the olfactory bulb and is required for axonal transport and fasciculation in olfactory sensory neurons, thus LIS1 deficiency disrupts olfactory bulb development and axon targeting [24].

In our previous study, we reported that JBTS17 depletion reduced LIS1 protein and impaired neuronal migration during corticogenesis [13]. Building on this, we prepared mouse embryonic fibroblasts (MEFs) from *Jbts17*^{KO} and wild-type embryos and performed immunoblotting for Lis1 with GAPDH as a loading control. Lis1 levels were reduced in *Jbts17*^{KO} MEFs relative to wild type (Fig. 2C). These findings extend the Jbts17-LIS1 relationship to a germline knockout context and provide a robust cell-level readout of Jbts17 deficiency. While we did not measure Lis1 directly in brain tissue here, the reduction observed in *Jbts17*^{KO} MEFs is consistent with a mechanism that could contribute to the cortical thinning and bilateral olfactory nerve agenesis documented in Jbts17-deficient embryos. We note that due to loss of original samples, densitometric quantification could not be performed. Thus, immunoblot data of Fig. 2C should be considered qualitative evidence of reduced Lis1 levels in Jbts17-deficient MEFs.

DISCUSSION

This study delineates an anatomically coherent spectrum of ciliopathy type phenotypes in Jbts17 deficient mice and relates them to developmental contexts in which primary cilia provide essential patterning information. Across systems, we observe regionally restricted structural anomalies, such as ocular hypopigmentation with optic cup shallowing, anterior craniofacial dysmorphology, autopod restricted polydactyly, and forebrain involvement marked by cortical plate thinning with qualitative ventriculomegaly and bilateral olfactory nerve agenesis, despite preserved overall somatic and telencephalic size at late gestation. The convergence of these findings supports the view that Jbts17 is required for cilia dependent morphogenesis in multiple embryonic fields.

Beyond ciliary assembly, JBTS17 has also been implicated at the centrosome and basal body, where it may interface with LIS1-dynein related processes. Such extraciliary functions provide a plausible mechanism by which loss of Jbts17 could influence spindle positioning, interkinetic nuclear migration, and axonal transport, potentially compounding cilia mediated patterning defects. Although we did not assess LIS1 distribution in neural tissue, this axis represents an interpretive but not demonstrated link between JBTS17 and neurodevelopmental outcomes.

The limb phenotype is instructive. Autopod restricted, bilateral but asymmetric polydactyly with a predominance of postaxial elements, together with a preaxial bifid ray in one autopod, is a classic signature of impaired Sonic hedgehog interpretation in the developing limb bud. In normal development, primary cilia on limb mesenchyme mediate GLI processing downstream of Sonic hedgehog from the zone of polarizing activity [7,20]. Perturbation of this ciliary relay skews the anteroposterior program and yields extra distal elements [7]. The pattern we document—supernumerary rays lateral to digit V with preserved stylopod and zeugopod proportions—fits within this framework and aligns with polydactyly reported in JBTS17 loss-of-function cohorts in the Joubert spectrum and oral facial digital syndrome type VI [16,25-27].

In the craniofacial domain, narrowing of the external nares and midface flattening implicate derivatives of the frontonasal and maxillary prominences, tissues whose growth and fusion are tightly coupled to cilia dependent signals, including Sonic hedgehog and WNT planar cell polarity pathways [28,29]. The ocular hypopigmentation and optic cup shallowing likewise map to a cilia sensitive compartment of eye morphogenesis, in keeping with variably penetrant retinal findings in ciliopathy patients and with observations in other ciliary gene mutants [19]. Notably, overall body size was preserved at E18 and P0, which emphasizes that the dominant consequence of Jbts17 loss is regional patterning failure rather than global growth restriction.

Forebrain findings extend this theme. Although whole mount brains were comparable in size and contour, coronal sections revealed cortical plate thinning in the dorsal telencephalon together with an apparent expansion of the lateral ventricular space. This combination suggests reduced radial output of cortical progenitors while tangential dimensions remain relatively preserved at this stage. Primary cilia on radial glia and intermediate progenitors are known to tune proliferative dynamics and fate decisions through morphogen input. Compromised ciliary transduction would be expected to blunt radial growth and could secondarily manifest as relative ventriculomegaly [8,9]. In the same embryos, we observed bilateral agenesis of the olfactory nerve at the level of the fila olfactoria, with no discernible bundles bridging the nasal cavity to the forebrain, indicating a failure of rostral forebrain to nasal connectivity near the time when olfactory sensory axons normally traverse the cribriform plate. Because both olfactory sensory neurons and forebrain targets depend on cilia related signaling and guidance milieus, this loss of connectivity fits a cilia-centered model [30]. Importantly, our prior siRNA mediated depletion studies did not reveal olfactory nerve agenesis, whereas the knockout did. This difference may reflect stronger and earlier loss of function in the germline null context and reveals a broader neurodevelopmental spectrum.

At the cellular level, we add an independent line of evidence by showing that Lis1 protein is reduced in *Jbts17*^{KO} mouse embryonic fibroblasts, recapitulating our earlier report that JBTS17 depletion lowers LIS1 and perturbs neuronal migration during corticogenesis. LIS1 (PAFAH1B1) is a core dynein regulator that supports mitotic spindle positioning, interkinetic nuclear migration, and neuronal migration; dosage reduction produces thinner and disorganized cortex and impairs axonal transport and fasciculation in olfactory pathways [22,23]. In principle, loss of JBTS17 could alter LIS1 availability or localization to dynein complexes at the centrosome and basal body. Such changes would be expected to influence spindle orientation in progenitors, inter-

kinetic nuclear migration, and axon transport or fasciculation, which align conceptually with the cortical and olfactory phenotypes we report. Because we did not examine LIS1 distribution in brain tissue, these possibilities remain interpretive rather than demonstrated. We therefore frame this as compatibility rather than proof of a direct causal chain within forebrain tissue view reduced Lis1 in Jbts17 null cells as a cell level correlate that is compatible with the anatomical phenotype, not as proof of a direct causal chain in the forebrain.

Several features strengthen the model. First, both alleles introduce early N terminal frameshifts that are predicted to create premature stop codons, providing a stringent loss-of-function context. Second, the phenotypes are anatomically clear at late gestation and birth and reproducible across organ systems that are classically affected in ciliopathies. Third, the Lis1 reduction furnishes a convenient cell level readout of Jbts17 deficiency that can anchor future mechanistic work on the Jbts17 LIS1 axis.

While our observations across eye, craniofacial, limb, and forebrain structures are compatible with impaired ciliary signaling in Jbts17 deficiency, the present data do not establish a direct causal chain between loss of Jbts17, altered ciliary function, and the reduction of Lis1. We therefore interpret the findings as supportive but not definitive evidence of a Jbts17-Lis1 connection. Several limitations temper this interpretation. First, we did not perform skeletal preparations or micro-CT imaging to assign digit identity or duplication levels. Second, cortical thickness and ventricular size were assessed qualitatively rather than by quantitative morphometrics. Third, we did not examine ciliary markers such as ARL13B or acetylated tubulin, nor did we measure SHH-GLI pathway readouts (Gli1, Ptch1, GLI3A/GLI3R) in embryonic tissues. Fourth, the olfactory pathway was not studied with OMP or GAP43 labeling, tract volumetry, or axon tracing. Finally, Lis1 measurements were limited to MEFs and were not extended to brain tissue. Importantly, no additional experiments can be performed because the original samples and mouse line are no longer available. We therefore outline future directions for the field rather than claims supported by our data, including tissue level ciliary and pathway readouts, quantitative morphometrics, and cellular rescue strategies that test whether restoring LIS1 or compensating dynein related functions can mitigate neurodevelopmental defects in appropriate model systems.

In sum, early truncating Jbts17 alleles produce ocular and anterior craniofacial defects, autopod restricted polydactyly, and forebrain anomalies marked by cortical thinning and olfactory nerve agenesis, while Lis1 is reduced in Jbts17 null cells. These findings position Jbts17 as a contributor to cilia dependent patterning across limb and forebrain and establish a practical mouse model that couples clear anatomical readouts with tractable cellular assays. By integrating regional patterning defects with preserved overall growth, this model provides a useful platform for quantitative skeletal mapping and tissue level mechanistic studies that can bridge anatomy to molecular pathogenesis in JBTS17 related ciliopathies.

REFERENCES

1. Bangs F, Anderson KV. Primary cilia and mammalian hedgehog signaling. Cold Spring Harb Perspect Biol. 2017;9.
2. Zhang K, Da Silva F, Seidl C, Wilsch-Bräuninger M, Herbst J, Huttner WB, et al. Primary cilia are WNT-transducing organelles whose biogenesis is controlled by a WNT-PP1 axis. Dev Cell. 2023;58:139-54.e8.
3. Clement DL, Mally S, Stock C, Lethan M, Satir P, Schwab A, et al. PDGFRα signaling in the primary cilium regulates NHE1-dependent fibroblast migration via coordinated differential activity of MEK1/2-ERK1/2-p90RSK and AKT signaling pathways. J Cell Sci. 2013;126:953-65.
4. Brugmann SA, Cordero DR, Helms JA. Craniofacial ciliopathies: a new classification for craniofacial disorders. Am J Med Genet A. 2010;152a:2995-3006.
5. Handa A, Voss U, Hammarsjö A, Grigelioniene G, Nishimura G. Skeletal ciliopathies: a pattern recognition approach. Jpn J Radiol. 2020;38:193-206.
6. Lee JE, Gleeson JG. Cilia in the nervous system: linking cilia function and neurodevelopmental disorders. Curr Opin Neurol. 2011;24:98-105.
7. Tickle C, Towers M. Sonic Hedgehog signaling in limb development. Front Cell Dev Biol. 2017;5:14.
8. Willaredt MA, Tasouri E, Tucker KL. Primary cilia and forebrain development. Mech Dev. 2013;130:373-80.
9. Hasenpusch-Theil K, Theil T. The multifaceted roles of primary cilia in the development of the cerebral cortex. Front Cell Dev Biol. 2021;9:630161.
10. Guo J, Otis JM, Suciu SK, Catalano C, Xing L, Constable S, et al. Primary cilia signaling promotes axonal tract development and is disrupted in Joubert Syndrome-Related Disorders models. Dev Cell. 2019;51:759-74.e5.
11. Wang H, Li Y, Li X, Sun Z, Yu F, Pashang A, et al. The primary cilia are associated with the axon initial segment in

neurons. Adv Sci. 2025;12:2407405.
12. Toriyama M, Lee C, Taylor SP, Duran I, Cohn DH, Bruel AL, et al. The ciliopathy-associated CPLANE proteins direct basal body recruitment of intraflagellar transport machinery. Nat. Genet. 2016;48:648-56.
13. Hong H, Joo K, Park SM, Seo J, Kim MH, Shin E, et al. Extraciliary roles of the ciliopathy protein JBTS17 in mitosis and neurogenesis. Ann Neurol. 2019;86:99-115.
14. Damerla RR, Cui C, Gabriel GC, Liu X, Craige B, Gibbs BC, et al. Novel Jbts17 mutant mouse model of Joubert syndrome with cilia transition zone defects and cerebellar and other ciliopathy related anomalies. Hum Mol Genet. 2015;24:3994-4005.
15. Wentzensen IM, Johnston JJ, Keppler-Noreuil K, Acrich K, David K, Johnson KD, et al. Exome sequencing identifies novel mutations in C5orf42 in patients with Joubert syndrome with oral-facial-digital anomalies. Hum Genome Var. 2015;2:15045.
16. Bonnard C, Shboul M, Tonekaboni SH, Ng AYJ, Tohari S, Ghosh K, et al. Novel mutations in the ciliopathy-associated gene CPLANE1 (C5orf42) cause OFD syndrome type VI rather than Joubert syndrome. Eur J Med Genet. 2018;61:585-95.
17. Asadollahi R, Strauss JE, Zenker M, Beuing O, Edvardson S, Elpeleg O, et al. Clinical and experimental evidence suggest a link between KIF7 and C5orf42-related ciliopathies through Sonic Hedgehog signaling. Eur J Hum Genet. 2018;26:197-209.
18. Zeng H, Ali S, Sebastian A, Ramos-Medero AS, Albert I, Dean C, et al. CPLANE protein INTU regulates growth and patterning of the mouse lungs through cilia-dependent Hh signaling. Dev Biol. 2024;515:92-101.
19. Chen HY, Welby E, Li T, Swaroop A. Retinal disease in ciliopathies: recent advances with a focus on stem cell-based therapies. Transl Sci Rare Dis. 2019;4:97-115.
20. Quadri N, Upadhyai P. Primary cilia in skeletal development and disease. Exp Cell Res. 2023;431:113751.
21. Chou FS, Li R, Wang PS. Molecular components and polarity of radial glial cells during cerebral cortex development. Cell Mol Life Sci. 2018;75:1027-41.
22. Schwamborn JC, Knoblich JA. LIS1 and spindle orientation in neuroepithelial cells. Cell Stem Cell. 2008;2:193-4.
23. Gambello MJ, Darling DL, Yingling J, Tanaka T, Gleeson JG, Wynshaw-Boris A. Multiple dose-dependent effects of Lis1 on cerebral cortical development. J Neurosci. 2003;23:1719-29.
24. Royal SJ, Gambello MJ, Wynshaw-Boris A, Key B, Clarris HJ. Laminar disorganisation of mitral cells in the olfactory bulb does not affect topographic targeting of primary olfactory axons. Brain Res. 2002;932:1-9.
25. Egger J, Bellman MH, Ross EM, Baraitser M. Joubert-Boltshauser syndrome with polydactyly in siblings. J Neurol Neurosurg Psychiatry. 1982;45:737-9.
26. Ben-Salem S, Al-Shamsi AM, Gleeson JG, Ali BR, Al-Gazali L. Mutation spectrum of Joubert syndrome and related disorders among Arabs. Hum Genome Var. 2014;1:14020.
27. Shawky RM, Elabd HSAE, Gad S, Gamal R, Mohammad SA. Oral-facial-digital syndrome type VI with self mutilations. Egypt J Med Hum Genet. 2014;15:399-403.
28. Yamaguchi H, Meyer MD, Barrell WB, Faisal M, Berdeaux R, Liu KJ, et al. The primary cilia: orchestrating cranial neural crest cell development. Differentiation. 2025;142:100818.
29. Janečková E, Feng J, Guo T, Han X, Ghobadi A, Araujo-Villalba A, et al. Canonical Wnt signaling regulates soft palate development by mediating ciliary homeostasis. Development. 2023;150.
30. Joiner AM, Green WW, McIntyre JC, Allen BL, Schwob JE, Martens JR. Primary cilia on horizontal basal cells regulate regeneration of the olfactory epithelium. J Neurosci. 2015;35:13761-72.